**Title**
DEVELOPMENT OP A HELIUM-FILLED STREAMER CHAMBER SYSTEM



**Authors**
Stetz, Albert W.
Perez-Mendez, Victor.

**Publication Date**
1969-05-27

Submitted to Nuclear Instruments and Methods

UCRL-16891 Rev.
Preprint

cy. 2

# DEVELOPMENT OF A HELIUM-FILLED STREAMER CHAMBER SYSTEM



Albert W. Stetz and Victor Perez-Mendez

March 27, 1969

AEC Contract No. W-7405-eng-48



LAWRENCE RADIATION LABORATORY
UNIVERSITY of CALIFORNIA BERKELEY

cy. 2

UCRL-16891 Rev.

## DISCLAIMER

# DEVELOPMENT OF A HELIUM-FILLED STREAMER CHAMBER SYSTEM *

Albert W. Stetz and Victor Perez-Mendez

Lawrence Radiation Laboratory
University of California
Berkeley, California

## ABSTRACT

Development of a helium-filled streamer chamber system is described. Calculations of streamer formation are carried out to determine high voltage pulse requirements. It is found that a Marx generator is adequate to drive chambers of intermediate size if an image intensifier is used to view the streamers. A one-meter streamer chamber system employing a 350-kV Marx generator is described. This system was used in a recent cyclotron experiment to record $5 \times 10^5$ pictures with good resolution and reliability.

# I. INTRODUCTION

There has been considerable interest lately in using streamer chambers as alternatives to conventional bubble chambers for analyzing complex scattering events of high energy particles. It is hoped that the streamer chambers, which can be fired on command, many times a second, can overcome the limitations on counting rates and statistics that are inherent in bubble chamber operation. Many arrangements have been described,[1] but it may be fairly said that streamer chambers are still in their infancy.

Until now most streamer chambers have been filled with neon because of its low ionization potential and convenient spectrum. For many potential streamer chamber experiments, however, helium is necessary, or at least more convenient. They may be classed as follows:

1. Polarization experiments, which take advantage of the analyzing power of helium in nucleon-helium scattering.

2. High-energy particle-production experiments, which depend on the fact that helium is a tightly bound spin-zero isospin-zero nucleus to simplify the interpretation of the events.

3. Experiments in which the trajectories of very low-energy particles must be determined with a minimum of energy loss and multiple scattering.

In spite of their obvious advantages, helium streamer chambers are in several respects more difficult to operate than neon-filled chambers. For one thing, it is far more difficult to obtain reliable streamer formation in helium than in neon: a stronger electric field is required, and the width of the high-voltage pulse must be regulated more precisely. Another complication inherent in the sort of experiments described above is that

the streamer chamber must delineate tracks that differ greatly in specific ionization. Unfortunately, the rate of streamer development depends upon the original ionization density, so the ever-present difficulty of obtaining reliable streamer formation is compounded.

This article consists of an account of work done in developing a helium streamer chamber system for a proton-helium scattering experiment done at the 184-inch cyclotron at Berkeley. It contains some theoretical predictions for avalanche formation in helium, some high-voltage technology, and a description of the streamer chamber system itself.

## II. AVALANCHE DEVELOPMENT

### A. Basic Theory

In order to obtain adequate spatial resolution in streamer chambers it is necessary to limit electron multiplication along the trajectory of the ionizing particle to short primary avalanches. Fortunately this state of avalanche development can be studied quantitatively with the help of the well-known equations for electron mobility, diffusion, and Townsend multiplication.

The number of electrons in an avalanche is given by Townsend's law,

$$N = e^{\alpha x}, \qquad (1)$$

where $\alpha$ is the number of ions produced per centimeter of path length along the avalanche. It is a function of the pressure of the gas and the external field, as shown in Fig. 1. The avalanche length increases at a rate equal to the average velocity of a free electron in the field E. In helium the velocity and field are nearly proportional, with the constant of proportionality

or mobility constant,[2]

$$\mu = 7.6(10)^5 \frac{\text{cm/sec}}{\text{volts/cm-mm Hg}} .$$

As the electrons are swept forward in the electric field they also diffuse laterally. It can be shown[3] that if $N = \exp(\alpha x)$ electrons start at $x = 0$ at $t = 0$, then the number of electrons in the volume element $\Delta x \Delta y \Delta z$ after a time $t$ is

$$\Delta n = \frac{N}{(4 \pi Dt)^{3/2}} \exp \left[ - \frac{(x-vt)^2+y^2+z^2}{4Dt} \right] \Delta x \Delta y \Delta z, \qquad (2)$$

where $y$ and $z$ are coordinates perpendicular to the electric field and $D$ is the diffusion constant. $D$ also depends on the electric field; for a Maxwellian gas it is proportional to the average energy of the electrons and to the electron mobility,

$$D = \frac{2}{3} \mu U_{av}; \qquad (3)$$

for fields and pressures normally encountered in streamer chambers, $D$ is almost constant $\approx$ 10 volts.

As the avalanche increases in size, the attraction of the positive ion cloud on the faster-moving electron cloud becomes important. At some critical number of ion pairs it compensates exactly the external field, and the development of the avalanche stops. This would be the end of the story without some new mechanism to propagate the avalanche. Although the field is zero in the vicinity of the head, it is augmented in the region directly behind the electrons. As soon as a free electron is produced in this region by photo-ionization a new avalanche sprouts up. The electron multiplication proceeds much more rapidly in the high field, and the total region of ionization grows in a rapid, haphazard manner until it extends from the anode to

the cathode. This development is called the streamer phase.

There is almost no quantitative information available on photo-ionization processes in helium.[4] Presumably the metastable states of He at 19.5 eV are ionized by the photons from recombining $He^+$ ions. These photons have a maximum energy of 24.5 eV, which is far enough above threshold for the mechanism to be significant. We can expect photo-ionization cross sections two or three orders of magnitude below the electron ionization cross section. This corresponds to a mean free path for photons on the order of several centimeters. Observations of discharges in He streamer chambers show that the propagation of avalanches due to photo-ionization becomes noticeable in a time $t \lesssim 10$ nsec. If the high-voltage field persists longer than this, the streamers fan out along the field lines behind the initial avalanche, and the resolution of the tracks in the chamber deteriorates rapidly.

In order to use avalanche formation to delineate particle tracks it is desirable to stop electron multiplication just before the streamer phase sets in. The condition that the space charge exactly cancel the external field is called the Meek condition. This condition should be established as quickly as possible for the primary avalanches along the track. The electric field should then be shut off as quickly as possible before secondary avalanches become noticeable.

With the help of a simple model of avalanche formation, we investigate in the next section the interplay of the electric field, pulse width, and gas pressure in bringing about the Meek condition.

## B. Approximate Calculations

In order to calculate the space-charge field of the positive ions we

make the simplifying assumption that most of the ions are contained in a roughly circular region of radius $r = \sqrt{4Dt}$ at the head of the avalanche. The field at the boundary of this region due to the ions inside is

$$E_r = \frac{3N e}{32\pi\epsilon_0 \mu U_{av} t} , \tag{4}$$

where N is the number of ions in the avalanche, $\epsilon_0$ is the permittivity of free space, and Eq. (3) has been used to eliminate the diffusion constant. Both $\alpha$ and $U_{av}$ depend on the total field at the head of the avalanche, and as $E_r$ begins to cancel the external field, $\alpha$ decreases and the rate of streamer growth slows down. We can calculate approximately the various parameters at this stage of streamer development with a simple approximation: assume that $\alpha$, $U_{av}$, and the average electron velocity are constant for a time

$$t = x/\mu E , \tag{5}$$

until $E_r$ just equals the external field, whereupon the avalanche development stops. E is just the external electric field. From Eqs. (4) and (5) the Meek condition will be satisfied when

$$N = \frac{32\pi \epsilon_0 U_{av} x}{3e} . \tag{6}$$

Now assume we wish to operate a chamber with a spatial resolution equal to x along the direction of E. The total number of ions in each avalanche is given by Eq. (6). The first Townsend coefficient is then obtained by inverting Eq. (1), and the external field required to sustain this value is obtained from Fig. 1. Finally, the duration of the external field equals the time t given by Eq. (5). Some useful values for x, N, E, and t are

listed for various gas pressures in Table I.

Table I. Selected parameters at various gas pressures.

| x (mm) | Pressure (atm) | N | E (kV/cm) | t (nsec) |
|---|---|---|---|---|
| 1 | 1 | $1.8(10)^7$ | 19 | 5 |
| 1 | 2 | $1.8(10)^7$ | 27 | 7 |
| 1 | 0.5 | $1.8(10)^7$ | 15 | 3 |
| 0.5 | 1 | $9.2(10)^6$ | 29 | 2 |
| 0.5 | 2 | $9.2(10)^6$ | 38 | 3 |
| 0.5 | 0.5 | $9.2(10)^6$ | 25 | 1 |
| 2 | 1 | $3.7(10)^7$ | 13 | 15 |
| 2 | 2 | $3.7(10)^7$ | 20 | 20 |
| 2 | 0.5 | $3.7(10)^7$ | 10 | 10 |

The number of photons emitted by an avalanche may be estimated as follows.[3] It is usually assumed that the number of photons created between t and t+dt:P(t) is proportional to the total number of drifting electrons and to the path length,

$$dP(t) = \delta\, N(t)\, v\, dt,$$

where $\delta$ is the number of photons produced by one electron per centimeter. From Eq. (1),

$$dN(t) = \alpha\, N(t)\, v\, dt\ ,$$

so

$$dP(t) = Q\, dN(t)\ ,$$

where $Q = \delta/\alpha$ is the photon efficiency per ionizing collision and depends on the gas, the external field, and the pressure. It has been determined experimentally that Q is a number on the order of unity for most gases at

atmospheric pressure. Moreover, $\delta$ is practically independent of E, so that Q decreases with increasing field as $\alpha$ increases.

This brings us to the following points regarding the design of streamer chamber equipment.

1. The number of photons emitted per avalanche depends mostly on the length the avalanches are allowed to attain. Increasing the chamber voltage decreases the number of ion pairs as well as the number of photons emitted per ion.

2. The light produced by $10^7$ electrons is not sufficient to be photographed with ordinary techniques. (Roughly 100 photons are required to expose a single grain in a sensitive emulsion.) For photographing tracks with reasonable demagnification, a total gain of 10 to 100 in light intensity suffices. The gain can be provided by any one of various commercially available two- and three-stage image intensifier tubes, which provide a nominal gain in light intensity of 5000 to 30 000. This gain, offset by the light losses encountered in coupling the output of the image tube to the film, is sufficient for most applications.

3. For a given spatial resolution and luminosity, increasing the gas pressure lengthens the time interval in which the avalanche forms and increases the voltage required to form it. For example, it would require about three times as much energy to drive a chamber if the pressure were doubled.

## III. HIGH VOLTAGE TECHNOLOGY

It is obvious from the foregoing calculations that useful streamer chambers require voltage sources on the order of hundreds of kilovolts and pulse widths of several nanoseconds. The Marx generator is the basis of

many such high-voltage systems, but various refinements are necessary to obtain satisfactory pulse shaping. Marx generators consisting of only a few stages can be built with rise times of 2 to 4 nsec, and these can be used to drive small chambers directly. Larger chambers and larger generators require some system to decrease the rise time of the pulse arriving at the chamber.

## A. The Marx Generator

Imagine an idealized Marx generator consisting of n capacitors charged to voltage $V_0$ and connected in series with spark gaps. A typical arrangement is shown in Fig. 2. To trigger the discharge, the first gap is overvoltaged from a third electrode. When this gap has become conductive, the voltage on the first capacitor is divided among the n-1 remaining gaps so that the second gap is overvoltaged by an amount $V_0/(n-1)$. The transit time required by a pulse to propagate along the system is small; the remaining gaps break down essentially simultaneously under the influence of the initial overvoltage.

The time required for these gaps to become conductive (and therefore the rise time of the output pulse) depends critically on the voltage $V_0 + V_0/(n-1)$. In practice, the resistance of the arc decreases from infinity to a negligibly low value in a few nanoseconds, depending on the applied voltage, the source impedance, and the gas density. Reference 1 quotes an empirical expression for the duration of the time-dependent resistance in spark gaps,

$$\tau_r = \frac{88}{Z^{1/3}E^{4/3}}(\rho/\rho_0)^{1/2} \text{ nsec},$$

where Z is the impedance of the voltage source, E is the electric field in

units of 10 kV/cm, $\rho$ is the density of the gas, and $\rho_0$ is the density of air at standard temperature and pressure.

After the resistive phase the combined inductance of the spark and its associated conductors may have an appreciable effect on the rise time of the generator output. The inductance of the spark is usually on the order of 1 to 2 nanohenries. The inductances of the conductors must be calculated from their geometry.

It is clear that the rise time of a Marx generator with many stages must be increased, not only from the inductance, which increases roughtly in proportion to the number of stages, but also from the increased spark formation time (since the overvoltage on each gap is proportional to $(n-1)^{-1}$). So it is that many-stage generators usually require some external pulse-shaping circuit to obtain adequate rise times. An arrangement such as the Blumlein involving switched transmission-line segments is probably necessary for very large chambers. Smaller chambers such as the one described below can be driven directly from the output of the Marx generator.

## B. Chamber Construction

In most experimental applications, the capacitance and inductance of the chamber conspire to distort the high-voltage pulse badly unless some care is taken to operate the chamber as part of a terminated transmission line. Generally speaking, the configuration of two long parallel conducting strips behaves like a transmission line of impedance $Z_0 = 377$ (spacing/width) ohms. A pulse propagates along such a line without distortion until it encounters some discontinuity. If the shape of the strip line changes abruptly, some fraction of the pulse is reflected, and the wave shape in

the preceding section is distorted. With large chambers, the following steps have to be taken:

First, the chamber should be part of a strip line which is terminated in its characteristic impedance. Reliable terminating resistors for high frequency and voltage application can be made from $CuSO_4$ electrolyte and copper electrodes.

Second, all changes of shape of the transmission line should be made gradually, and preferably upstream from the chamber. Usually the line is fed from some high-impedance source like a spark gap. In order to transfer as much energy as possible, the line should be smoothly flared from its input to the region of the chamber.

The chamber itself is just a transparent insulating box. The electrodes should not come into contact with the gas in the chamber at any point. The inside of the chamber should be as smooth as possible. These steps must be taken to reduce the spurious discharges and flares that occur around any discontinuity in the electric field.

The electrodes have to be as conductive as possible and yet transparent. Coarse, hand-woven mesh seems to be ideal. Expanded metal mesh, which is as much as 94% transparent, is available in limited widths.

Finally, during actual operation the helium quickly becomes contaminated. The light produced by the streamers is quite sensitive to the quenching effect of hydrocarbon molecules, consequently the gas in the chamber must be circulated rapidly to maintain consistent operation.

## C. Design of a Small Streamer Chamber System

The foregoing techniques were used in constructing a small streamer

chamber for a double-scattering experiment in which a polarized beam of protons was allowed to scatter on helium nuclei inside the active volume of the chamber. It was desired that the system operate reliably over many hours of cyclotron time, and provide good resolution of simultaneous tracks differing vastly in ionization density. The scattering events were constrained to lie approximately in the horizontal plane, so that stereo photography was not attempted, and resolution parallel to the electric field was not important.

The heart of the system is a seven-stage Marx generator constructed at the Lawrence Radiation Laboratory for use with streamer chambers with 4- to 8-in. gaps. The circuit diagram is shown in Fig. 2. The first stage consists of a three-electrode gap overvoltaged with a 30-kV pulse applied to the gap through a needle electrode. This trigger pulse is generated with a conventional spark-gap trigger amplifier, and stepped up in voltage by a factor of 3 by a pulse transformer.

Each subsequent stage consists of four $BaTiO_2$ capacitors with a net (nominal) capacitance of 3900 pF and 60 kV maximum working voltage. The switching gaps are 0.5-in. brass balls operated in nitrogen at 5 to 7 atm pressure. The physical layout is shown in Fig. 3. The 47-kΩ charging resistors are mounted on the side and the entire assembly is mounted in a pressurized tank.

The generator has typically been operated at 48 kV input voltage with gap spacing of 0.1 in. and 100 lb/in.$^2$ pressure. The output is 300 kV with a 10-nsec rise time into a 100-Ω load.

The chamber and the generator are shown in Fig. 4. The output of the Marx generator is flared out to a strip line 24 in. wide with 5.5-in.

electrode spacing. The line is terminated in 100 Ω near the downstream end. At the point where the line begins to flare, a parallel spark gap is placed to shape the falling edge of the high voltage pulse. This gap consists of 2-in. brass electrodes operated in dry nitrogen pressurized about 2 atm. No attempt is made to trigger this gap, but a source of ultraviolet light is flashed to liberate photoelectrons at the anode. These electrons stabilize the time of spark formation following the arrival of the high voltage pulse. The width of the pulse and consequently the length and luminosity of the streamers are controlled by changing the gap pressure and spacing.

The chamber itself is made with 10-mil Mylar walls and Lucite top and bottom pieces. It is filled with helium with about 0.1% alcohol vapor to reduce the memory time. A capacitive voltage probe was installed in the ground plane just prior to the chamber to monitor the waveform.

The chamber was photographed with the help of an RCA C70021 three-stage image intensifier tube. This tube has a 2.5-in. photocathode and anode, and is magnetically focused. It was run with a total accelerating voltage of 30 kV, about 10 kV per stage, and has a nominal gain of 20 000. The chamber was imaged on a 1-in.$^2$ area on the cathode by an f1.4 Nikon 50 mm lens. The light output is coupled to the film with a special Zeiss lens that provides 108 mm focal length at f1.2. With this optical arrangement we are able to resolve six line pairs per centimeter at the position of the chamber with no noticeable distortion. The effective gain in light intensity over a single f1.4 lens is about 30. The image is photographed with Kodak Tri-X film.

Some sample scattering events are shown in Fig. 5. The denser

tracks are recoil $\alpha$ particles stopping in the chamber. The fainter tracks are 80-MeV protons. It was found essential to operate the chamber near the threshold of streamer formation, otherwise the more densely ionized track becomes too broad and luminous to photograph and measure accurately. Stereo photography was not attempted.

## FOOTNOTE AND REFERENCES

* Work done under the auspices of the U. S. Atomic Energy Commission.

1. F. Bulos, A. Odian, F. Villa, and D. Yount, Streamer Chamber Development, Stanford Linear Accelerator Center Report-75, June 1967 (unpublished).

2. Sanborn C. Brown, Basic Data of Plasma Physics, First Edition (Massachusetts Institute of Technology Press, Cambridge, 1966).

3. H. Reather, Electron Avalanches and Breakdown in Gases (Butterworths, London, 1964).

4. L. B. Loeb, Basic Processes of Gaseous Electronics (University of California Press, Berkeley, 1961).

## FIGURE LEGENDS

Fig. 1. The first Townsend coefficient as a function of electric field for various gases. From Ref. 2.

Fig. 2. Circuit of seven-stage 350-kV Marx generator.

Fig. 3. Layout of Marx generator with several capacitors removed to show spark gaps.

Fig. 4. Chamber and transmission-line assembly.

Fig. 5. Proton-helium scattering events photographed with the image intensifier. (a) Elastic scattering. (b) An inelastic event, presumably pHe → ppt.

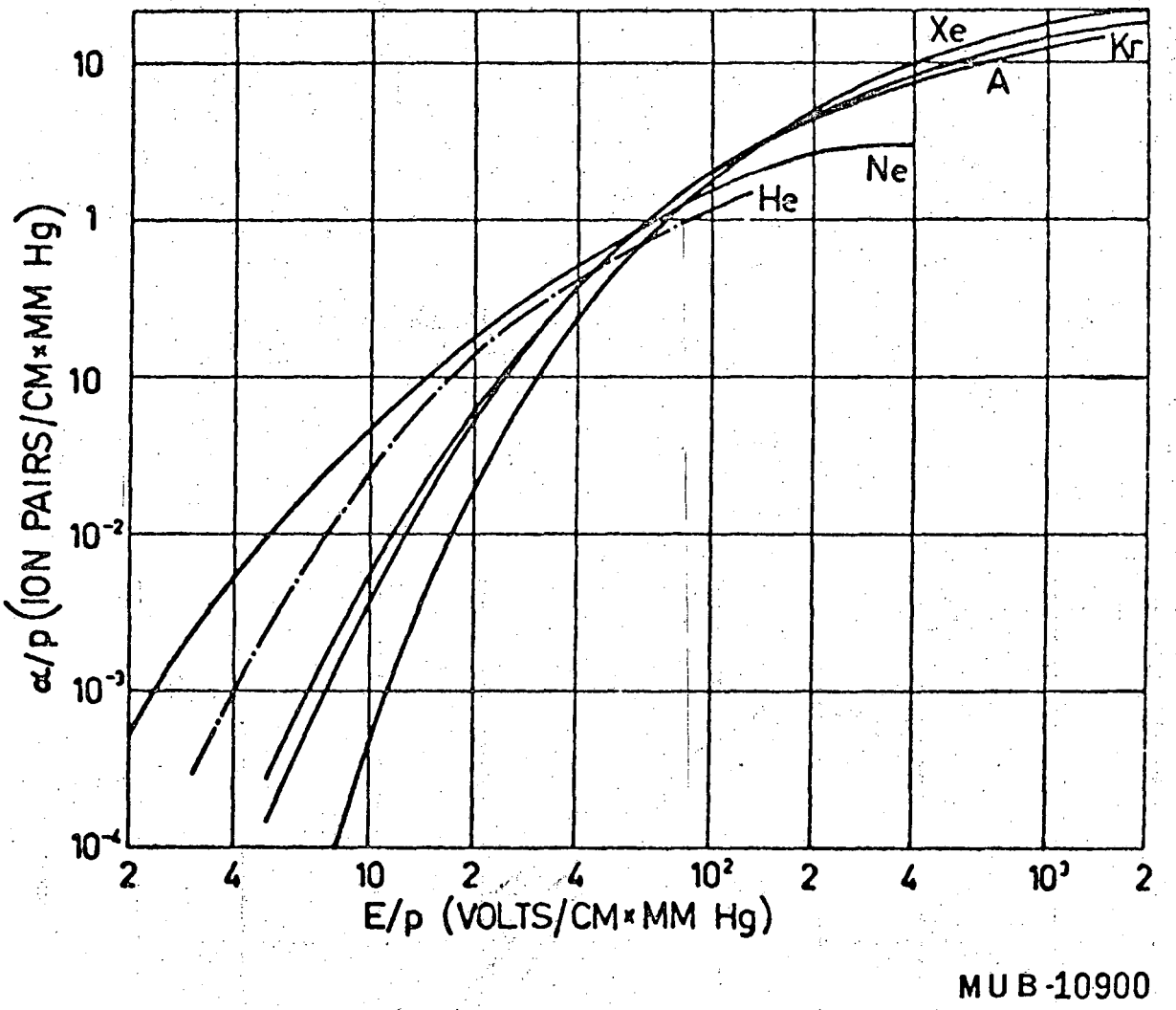
Xe
Kr
A
Ne
He
10
1
10
$10^{-2}$
$10^{-3}$
$10^{-4}$
α/p (ION PAIRS/CM×MM Hg)
2
4
10
2
4
$10^2$
2
4
$10^3$
2
E/p (VOLTS/CM×MM Hg)
MUB-10900

Fig. 1

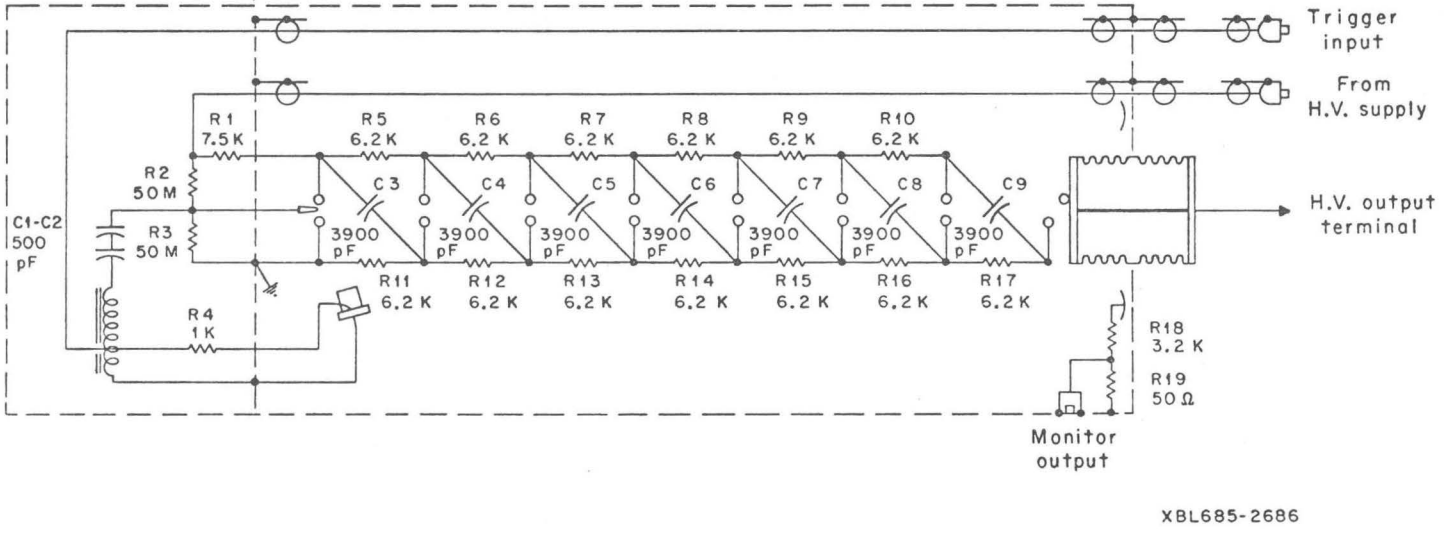
Trigger input
From H.V. supply
R1 7.5K
R5 6.2K
R6 6.2 K
R7 6.2 K
R8 6.2 K
R9 6.2 K
R10 6.2 K
R2 50 M
C3
C4
C5
C6
C7
C8
C9
C1-C2 500 pF
R3 50 M
3900 pF
H.V. output terminal
R11 6.2 K
R12 6.2 K
R13 6.2 K
R14 6.2 K
R15 6.2 K
R16 6.2 K
R17 6.2 K
R4 1K
R18 3.2 K
R19 50 Ω
Monitor output
XBL685-2686

Fig. 2

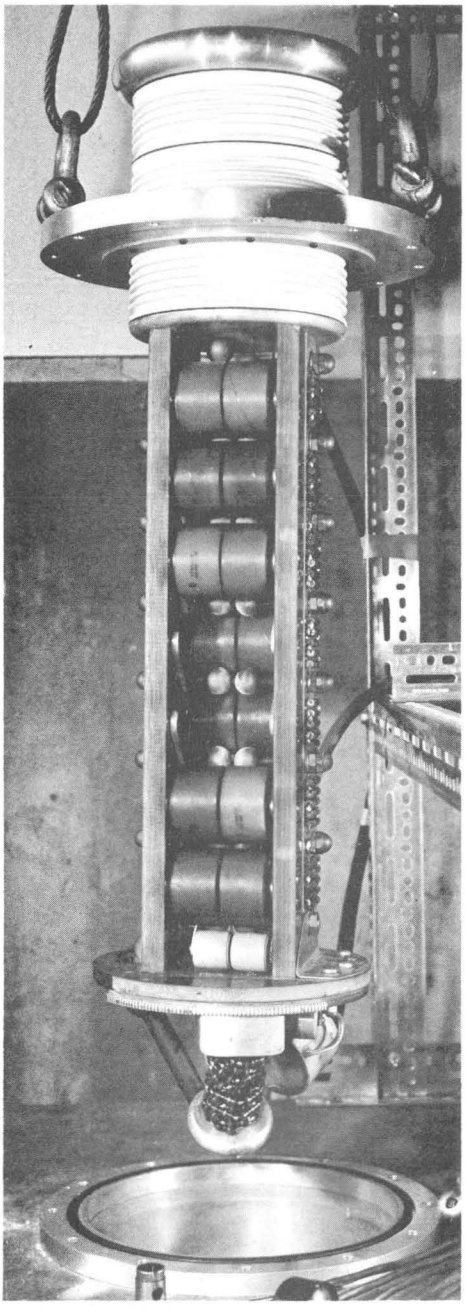

GPR-3142

Fig. 3

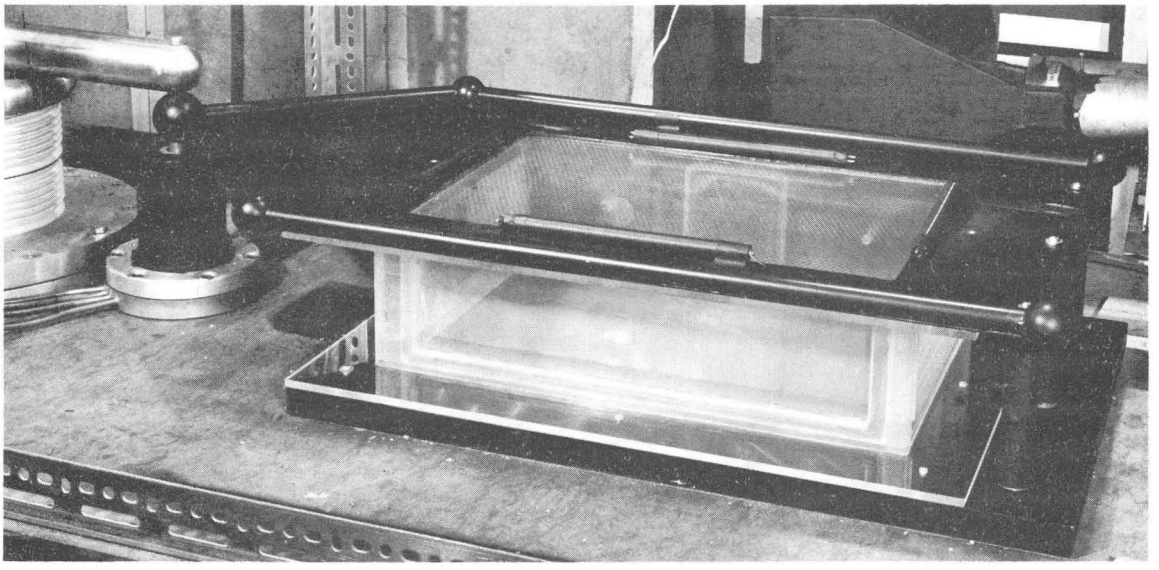

GPR-3141

Fig. 4

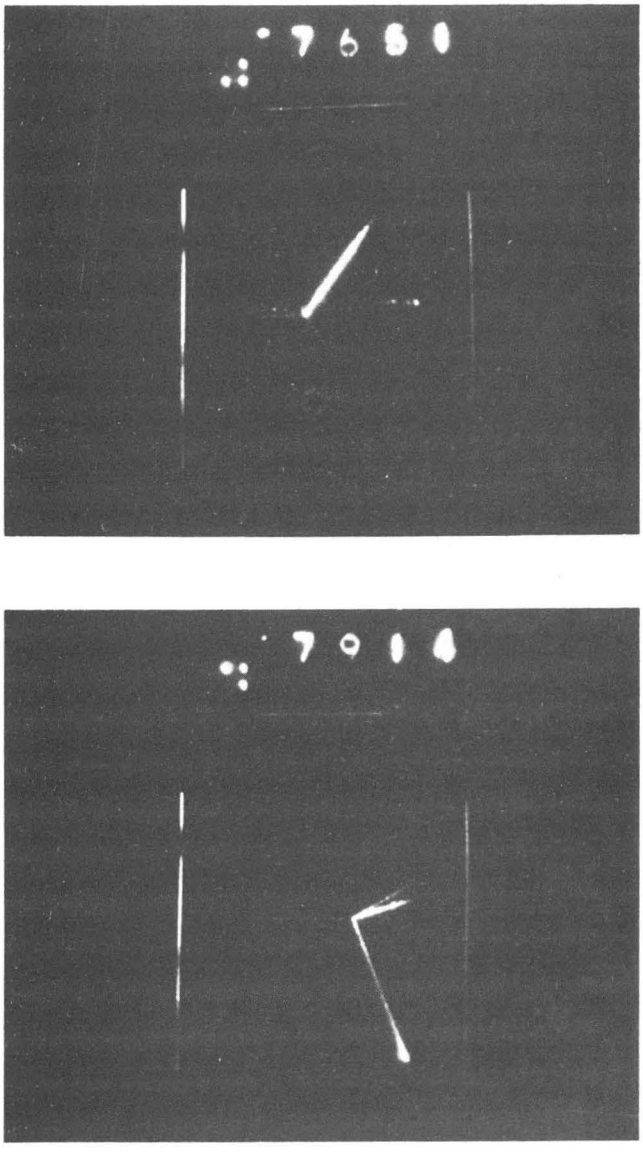


XBB 685-2895

Fig. 5

## LEGAL NOTICE

*TECHNICAL INFORMATION DIVISION*
*LAWRENCE RADIATION LABORATORY*
*UNIVERSITY OF CALIFORNIA*
*BERKELEY, CALIFORNIA 94720*